

Stable and wavelength-tunable silicon-micro-ring-resonator based erbium-doped fiber laser

L. G. Yang,¹ C. H. Yeh,² C. Y. Wong,³ C. W. Chow,^{1*} F. G. Tseng,⁴ and H. K. Tsang³

¹*Department of Photonics and Institute of Electro-Optical Engineering, National Chiao Tung University, Hsinchu 30010, Taiwan*

²*Information and Communications Research Laboratories, Industrial Technology Research Institute (ITRI), Hsinchu 31040, Taiwan*

³*Department of Electronic Engineering, The Chinese University of Hong Kong, Hong Kong*

⁴*Department of Engineering and System Science, National Tsing Hua University, Hsinchu 30013, Taiwan*

* cwchow@faculty.nctu.edu.tw

Abstract: In this work, we propose and demonstrate a stable and wavelength-tunable erbium-doped fiber (EDF) ring laser. Here, a silicon-on-insulator (SOI)-based silicon-micro-ring-resonator (SMRR) is used as the wavelength selective element inside the fiber ring cavity. A uniform period grating coupler (GC) is used to couple between the SMRR and single mode fiber (SMF) and serves also as a polarization dependent element in the cavity. The output lasing wavelength of the proposed fiber laser can be tuned at a tuning step of 2 nm (defined by the free spectral range (FSR) of the SMRR) in a bandwidth of 35.2 nm (1532.00 to 1567.20 nm), which is defined by the gain of the EDF. The optical-signal-to-noise-ratio (OSNR) of each lasing wavelength is larger than 42.0 dB. In addition, the output stabilities of power and wavelength are also discussed.

©2013 Optical Society of America

OCIS codes: (060.2320) Fiber optics amplifiers and oscillators; (060.3510) Lasers, fiber; (060.4510) Optical communications.

References and links

1. Y. J. Rao, Z. L. Ran, and R. R. Chen, "Long-distance fiber Bragg grating sensor system with a high optical signal-to-noise ratio based on a tunable fiber ring laser configuration," *Opt. Lett.* **31**(18), 2684–2686 (2006).
2. C.-H. Yeh, T.-T. Huang, H.-C. Chien, C.-H. Ko, and S. Chi, "Tunable S-band erbium-doped triple-ring laser with single-longitudinal-mode operation," *Opt. Express* **15**(2), 382–386 (2007).
3. Y. Yu, L. Lui, H. Tam, and W. Chung, "Fiber-laser-based wavelength division multiplexed fiber Bragg grating sensor system," *IEEE Photon. Technol. Lett.* **13**(7), 702–704 (2001).
4. S. Yamashita and M. Nishihara, "Widely tunable erbium-doped fiber ring laser covering both C-band and L-band," *IEEE J. Sel. Top. Quantum Electron.* **7**(1), 41–43 (2001).
5. C. H. Yeh and C. W. Chow, "Wavelength-selectable single-longitudinal-mode Fabry-Perot laser source using inter-injection mode-locked technique," *Opt. Fiber Technol.* **16**(5), 271–273 (2010).
6. M. A. Umyy, N. Madamopoulos, A. Joyo, M. Kouar, and R. Dorsinville, "Tunable multi-wavelength SOA based linear cavity dual-output port fiber laser using Lyot-Sagnac loop mirror," *Opt. Express* **19**(4), 3202–3211 (2011).
7. L. Xu, B. C. Wang, V. Baby, I. Glesk, and P. R. Prucnal, "Widely tunable fiber ring laser with EDFA/SOA," *Proc. of LEOS, 2001, Paper WC4*.
8. M. Krause, H. Renner, and E. Brinkmeyer, "Raman lasers in silicon photonic wires: unidirectional ring lasing versus Fabry-Perot lasing," *Electron. Lett.* **45**(1), 42–43 (2009).
9. B. Jalali and S. Fathpour, "Silicon photonics," *J. Lightwave Technol.* **24**(12), 4600–4615 (2006).
10. M. A. Popovic, T. Barwicz, M. R. Watts, P. T. Rakich, L. Socci, E. P. Ippen, F. X. Kärtner, and H. I. Smith, "Multistage high-order microring-resonator add-drop filters," *Opt. Lett.* **31**(17), 2571–2573 (2006).
11. D. Taillaert, W. Bogaerts, P. Bienstman, T. F. Krauss, P. Van Daele, I. Moerman, S. Verstuyft, K. De Mesel, and R. Baets, "An out-of-plane grating coupler for efficient butt-coupling between compact planar waveguides and single-mode fibers," *IEEE J. Quantum Electron.* **38**(7), 949–955 (2002).
12. X. Chen, C. Li, C. K. Y. Fung, S. M. G. Lo, and H. K. Tsang, "Apodized Waveguide Grating Couplers for Efficient Coupling to Optical Fibers," *IEEE Photon. Technol. Lett.* **22**(15), 1156–1158 (2010).
13. D. Taillaert, F. Van Laere, M. Ayre, W. Bogaerts, D. Van Thourhout, P. Bienstman, and R. Baets, "Grating couplers for coupling between optical fibers and nanophotonic waveguides," *Jpn. J. Appl. Phys.* **45**(8A), 6071–6077 (2006).
14. L. Zimmermann, H. Schröder, T. Tekin, W. Bogaerts, and P. Dumon, "g-Pack – a generic testbed package for silicon photonics devices," *Proc. Group IV Photonics* 371–373 (2008).

15. B. Liu, A. Shakouri, and J. E. Bowers, "Passive microring-resonator-coupled lasers," *Appl. Phys. Lett.* **79**(22), 3561–3563 (2001).
 16. T. Chu, N. Fujioka, S. Nakamura, M. Tokushima, and M. Ishizaka, "Compact, low power consumption wavelength tunable laser with silicon photonic-wire waveguide micro-ring resonators," *Proc. ECOC, 2009 Paper 7.2.1.*
-

1. Introduction

Stable and wavelength-tunable fiber ring lasers are attractive light sources for applications in wavelength-division-multiplexing (WDM) networks, optical testing and fiber sensing systems [1, 2]. Tunable bandpass filter (TBF), fiber Fabry-Perot tunable filters (FFP-TF) and fiber Bragg grating (FBG) have been used inside the fiber ring cavity to generate the tunable lasing wavelength [3–5]. Erbium-doped fiber amplifier (EDFA) or optical semiconductor amplifier (SOA) are usually used inside the fiber ring cavity as the gain-media [6, 7].

Silicon-micro-ring-resonator (SMRR) is an attractive optical component and it can be applied in various applications, such as wavelength multiplexing, optical switching, wavelength filtering and optical modulation [8, 9]. SMRR is usually based on silicon-on-insulator (SOI) structure, which is CMOS-compatible and cost-effective. Besides, the SMRR was also used to serve as a wavelength filter offering a 50-dB high extinct-ratio in a fiber laser system [10]. However, the optical power loss in the optical coupling between the single mode fiber (SMF) and the SMRR is a challenge issue, and this will reduce the output optical power and the stability of the fiber laser [11].

In this work, we propose and demonstrate a stable erbium-doped fiber (EDF) ring laser by using a SOI-based SMRR inside laser cavity for wavelength-tuning. Here, the free spectral range (FSR) of the SMRR is 2 nm. Thus, the output lasing wavelength of the proposed fiber laser can be tuned at a tuning step of 2 nm in a bandwidth of 35.2 nm (1532.00 to 1567.20 nm), which is defined by the gain of the EDF. The optical-signal-to-noise-ratio (OSNR) of each lasing wavelength is larger than 42.0 dB. The measured wavelength and power variation during the 30 min observation time are within 0.02 nm and 0.8 dB respectively.

2. Experiment and results

Figure 1(a) shows the experimental setup of the proposed wavelength-tunable EDF ring laser structure. This fiber laser was constructed by a commercially available C-band EDFA module, two polarization controllers (PCs), a 1×2 and 90:10 optical coupler (CP) and a SMRR with uniform-period grating coupler (GC). Figure 1(b) and 1(c) show the scanning-electron-microscope (SEM) images of SMRR with three ports (I: input-port, T: throughput-port, and D: drop-port) and the uniform-period GC, respectively. A basic add-drop configuration of proposed SMRR is also shown in Fig. 1(b). The GC shown in Fig. 1(c) has a coupling efficiency of about 30% between the SMF and the SMRR. The GC was a uniform-period shallow-etched grating without any overlay high-index layer or and additional reflectors.

By means of deep-ultra-violet (DUV) 193 nm lithography and reactive-ion etching (RIE) techniques, GCs and SMRR were fabricated on a SOI wafer with a 0.22 μm thick top silicon layer and a 2 μm thick BOX layer. The GCs have the length and width of 14 and 9 μm , respectively, while its period and etch depth are 580 and 70 nm, respectively. For the SMRR, the length of straight coupling region and the circumference are 6 and 232 μm , respectively. The gap between ring structure and the straight waveguide structure is 200 nm in the coupling region. Besides, the total length of straight waveguide structure is less than 1 cm

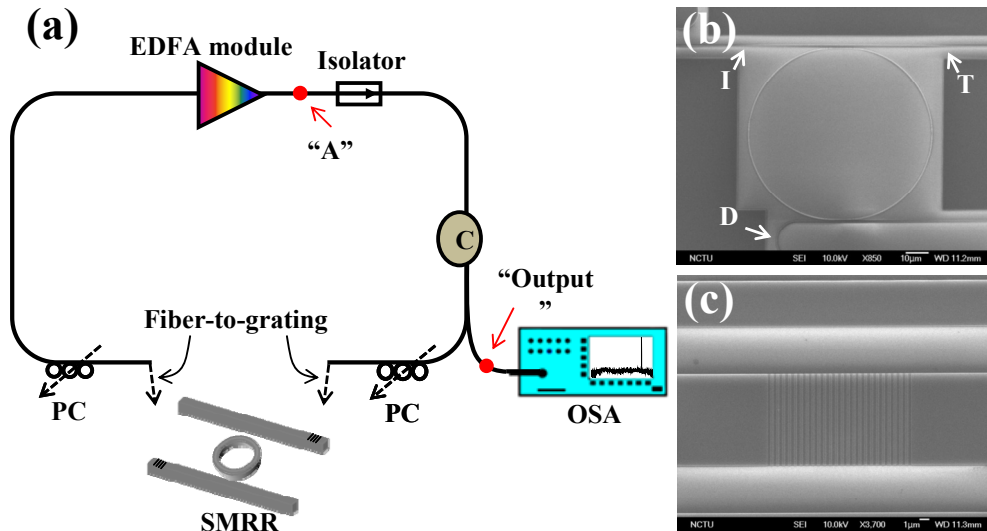


Fig. 1. (a) Experimental setup of proposed silicon photonics laser. The scanning-electron-microscope images of silicon-based devices for SMRR with (a) three ports (I: input-port, T: throughput-port, and D: drop-port) and (c) uniform-period grating coupler.

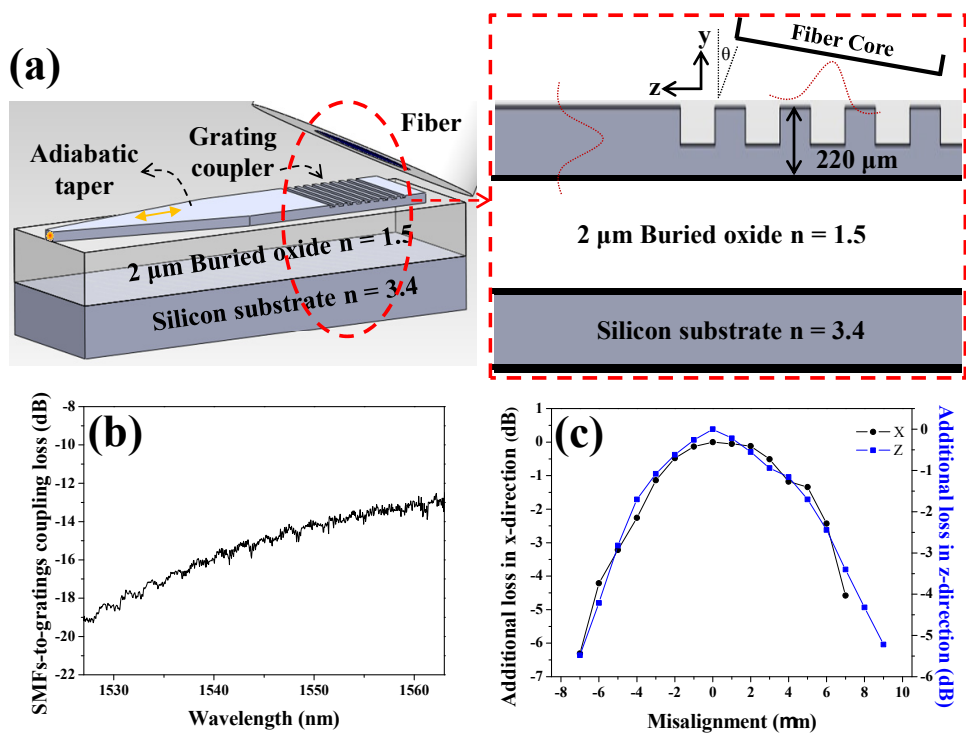


Fig. 2. (a) Schematic view of grating coupler on its tilt-view and side-view of grating coupler, (b) coupling loss (SMF-to-grating-to-SNW-to-grating-to-SMF), (c) misalignment tolerance in x-z plane.

We first describe the GC and its characteristic. Figure 2(a) shows the schematic view of grating coupler and the inset is side-view of GC. Light beam was launched from the SMF to the SMRR via the GC in the I-port, and then the light was coupled to the SMF via the GC in

the D-port. The GC structure was optimized for TE-polarization. As shown in the inset of Fig. 2(a), the incident angle of beam launching from the SMF has an off-vertical tilt angle of 10° to maximize the coupling efficiency. Vertical coupling is used in the measurement. There are several advantages of the vertical coupling [12, 13], such as large alignment tolerance, high flexibility to couple the optical signal to and from the SOI devices without dicing the chip, and simpler back-end processing without the requirement of facet polishing. A solution called “g-Pack” has been developed [14], which allows multiple optical input and output coupling between SMF and grating coupler with high mechanical stability, while the cost can be low. Figure 2(b) presents the fiber-to-fiber coupling loss (SMF-to-GC-to-straight silicon waveguide-to-GC-to-SMF). In the fiber-to-fiber coupling loss measurement, a continuous wave (CW) optical signal generated from a tunable laser was power boosted by an EDFA and then coupled into the silicon waveguide via the GC. Its wavelength was swept from 1520 nm to 1570 nm, and an optical power meter measured the output optical power. The measured fiber-to-fiber loss was -14 dB at 1565 nm, as shown in Fig. 2(b), and the loss is monotonously increasing from 1525.0 nm to 1565.0 nm. The power fluctuation at both ends of the spectrum is caused by the stop-band of the booster EDFA. Figure 2(c) shows the measured misalignment tolerance in x-z plane. It shows the misalignment tolerance in x and z directions are similar. Within the off-set range of ± 3 μm in x-z plane, the additional loss is under -1 dB.

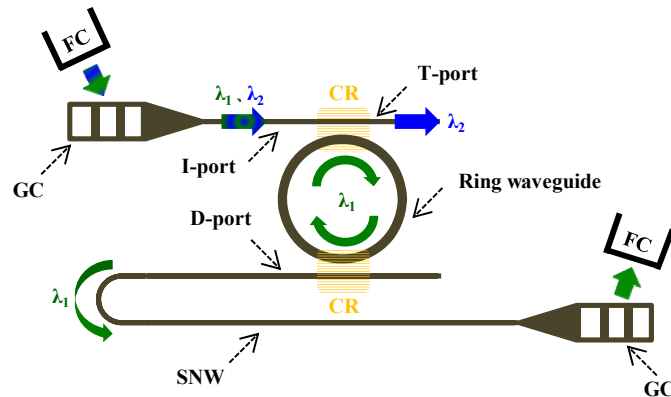


Fig. 3. Operation principle of fiber-to-waveguide and SMRR coupling (FC: fiber core; GC: grating coupler; CR: coupling region; SNW: straight nano-waveguide)

The SMRR comprised of two straight nano-waveguides (SNWs) and a ring waveguide. The SNW has a width of 500 nm and thickness of 220 nm, which offers good optical mode confinement. Figure 3 shows a simple diagram describing of SMRR operation mechanism. In order to avoid the Bragg second-order reflection, the launching light from the SMF should have an off-vertical tilt angle of 10° [12, 13]. The coupled optical mode was laterally tapered down to 500 nm through an adiabatic taper. Equation (1) describes the power transmission of a ring resonator [15]:

$$T_r = \frac{T_0}{1 + \left(\frac{2}{\pi} F\right)^2 \sin^2\left(\frac{\beta_r l_r}{2}\right)} \quad (1)$$

where T_0 is the transmission satisfying resonance condition (i.e. when $\beta_r l_r = N \times 2\pi$, N is an integer, β_r is the propagation constant in the SMRR, l_r is the circumference of the SMRR, and the FSR = $\lambda^2/n_r l_r$, n_r is the effective index of the ring waveguide. F is the finesse of the SMRR). For example, as it can be seen in Fig. 3, if λ_1 satisfies the resonance condition and hence will couple into the ring waveguide through evanescently side coupling. For other wavelengths not satisfying the resonance condition of the SMRR, for example λ_2 , it transmits directly to the T-port.

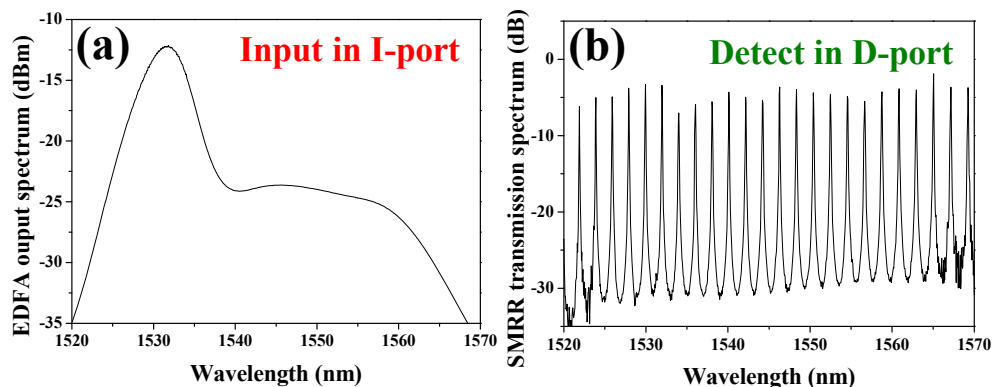


Fig. 4. (a) Output ASE spectrum of EDFA. (b) Output spectrum of SMRR with ~ 2 nm mode-spacing when ASE source is launched into I-port.

In the characterization of the SMRR, an amplified spontaneous emission (ASE) signal generated from an EDFA (shown in Fig. 4(a)) was coupled into the SMRR. Figure 4(b) shows the SMRR filtered output spectrum measured at D-port. The optical spectral was measured by an optical spectrum analyzer (OSA) with resolution of 0.01 nm. The maximum transmitted wavelengths are the wavelengths satisfying the resonant conditions of the SMRR, and the FSR is 2 nm as observed in Fig. 4(b).

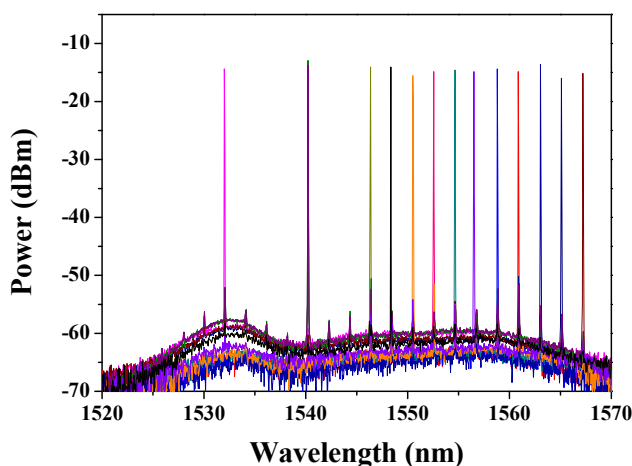


Fig. 5. Output spectra of the proposed fiber laser scheme in the wavelengths of 1532.0 to 1567.2 nm, when two PCs are properly adjusting.

The fiber laser was constructed as shown in Fig. 1(a). As mentioned before, the proposed laser structure consisted of a C-band EDFA module, two PCs, a 1×2 and 90:10 CP and a silicon-based SMRR. A polarization insensitive isolator was used in the fiber cavity allowing the optical signal to propagate in one direction. The 90:10 CP was used to tap out 10% of the optical in the proposed fiber laser. The EDFA with 5.8 dBm output power was used to act as the gain medium and two PCs are used for wavelength tuning, which can be done by manipulating the birefringent loss inside the laser system. Due to the different birefringent losses of proposed laser scheme, different lasing wavelengths can be generated as shown in Fig. 5. Thirteen lasing wavelengths can be tuned in the wavelengths range of 1532.00 to 1567.20 nm with a tuning step of 2.0 nm. The wavelength range and the tuning step are determined by the EDFA bandwidth and the FSR of the SMRR respectively. The optical spectrum and the output power were measured by using an OSA with a 0.01 nm resolution

and a PM respectively. In the measurement, some lasing mode cannot be generated, particularly at the shorter wavelength side. We believe it is due to the losses of GC and SMRR in these modes. Figure 5 also shows the lasing wavelength with a power difference of ± 1.5 dB over the 35.2 nm wavelength range. The average output power of each wavelength is 0.8 dBm. The OSNR of each lasing wavelength is larger than 42.0 dB.

By measuring the ratio of the output power of the proposed laser (measured at point “Output” in Fig. 1(a)) to the output power of the EDFA module (measured at point “A” in Fig. 1(a)), the power efficiency of the proposed laser is about 36%. Besides, we also measured the relationship between pumping current of the EDFA and the lasing power of the proposed laser. Figure 6(a) shows the measured slope efficiency of the proposed laser, which is about 0.02 W/A. This value is comparable with the value reported in the literature using semiconductor optical amplifier (SOA) and silicon micro-ring resonator [16].

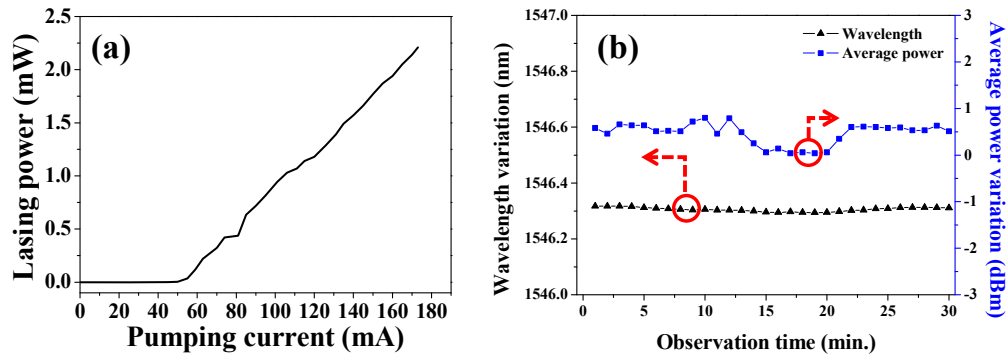


Fig. 6. (a) The slope efficiency of the proposed laser, and (b) output wavelength variation and fluctuation of output power in the proposed fiber laser under 30 minutes observation time, when the lasing light is set at 1546.32 nm initially.

In order to realize the stabilities of output power and wavelength of the proposed ring laser, a short-term observation was measured. The lasing wavelength of 1546.32 nm was selected for the measurement. As shown in Fig. 6(b), the measured wavelength and power variation during the 30 min observation time are within 0.02 nm and 0.8 dB, respectively. Moreover, during one hour observation, the measured output power and wavelength of the proposed fiber laser can still be maintained.

4. Conclusion

We proposed and demonstrated experimentally a stable and wavelength-tunable SMRR-based EDF ring laser. In order to enhance the coupling efficiency between the SMRR and the SMF, GC structure was used. In this work, we discussed and characterized the GC and SMRR. We also discussed the operation principle of the proposed wavelength-tunable fiber laser. The output lasing wavelength of the proposed fiber laser can be tuned at a tuning step of 2 nm (defined by the FSR of the SMRR) in a bandwidth of 35.2 nm (1532.00 to 1567.20 nm), which was defined by the gain of the EDF. The OSNR of each lasing wavelength was large than 42.0 dB. The output power difference was ± 1.5 dB over the 35.2 nm wavelength range. Moreover, the wavelength variation and power fluctuation could be observed within 0.02 nm and 0.8 dB, respectively, over 30 minutes observing time.

Acknowledgments

This work was financially supported by the National Science Council, Taiwan, R.O.C., under Contract NSC-101-2628-E-009-007-MY3 and NSC-100-2221-E-009-088-MY3.